

Permeability Measurements of Strained Fibrous Networks

Abstract Textiles are used in many industrial applications. For example, they are used in paper-making. Indeed, during the pressing of paper, felts are used to transport the wet paper web and to recover the water expressed from the wet sheet. To improve this operation, felt permeability has to be characterised. This property does depend on the fiber diameter and the whole structure, which is constituted of a base and a batt. Moreover, the different fibers may be mechanically entangled in order to improve the directional permeabilities. This paper describes the equipment developed to measure water permeability of fibrous media. Next, experimental results of felt samples are presented. The investigation on felt permeability tensor allows improvements in both felt design and process modeling. After a brief introduction, this paper is divided into four parts. The first one focuses on the presentation of the experimental device used for the permeability measurements. The second deals with the description of the experimental protocol. Results and discussion are presented in the third part. Finally, a conclusion will end this paper.

Key words fabrics/textiles, porosity, permeability, anisotropy, measurement

X. Thibault

ESRF BP 220 38043 Grenoble Cedex 09 France

J.-F. Bloch¹

EFPG BP 65 38402 St-Martin-d'Hères Cedex France

Introduction

Fibrous networks are encountered in many industries for different applications. We present in this paper both the experimental device and results concerning given woven structures that may be applied to different industrial applications. However, we will focus our attention on paper-making. Paper pulp contains roughly 95% water and only 5% of fiber mass. Therefore, the main purpose of each unit operation of a paper machine is to remove water from the wet fibrous network. Initially, the paper pulp is laid on a fabric, and the suspension is concentrated by filtration. The drainage is improved by depressor elements such as vacuum boxes in contact with the fabric. Next, the sheet

supported by the felt is pressed between rolls. Finally, the wet sheet is dried by heated rolls to remove the excess water and to reach a dryness ratio of 0.95 (ratio of dry and humid masses). The energy necessary to remove the same quantity of water by drying may be as much as six times higher than by pressing. Hence, for obvious economic purposes, each section of a paper machine has to be optimised. To achieve this aim, the transfer mechanisms that occur in each section, have to be understood. Our work deals here with the press section. When passing through

¹ Corresponding author: EFPG BP65 38402 St-Martin-d'Hères, Cedex France; email: jean-francis.bloch@efpg.inpg.fr

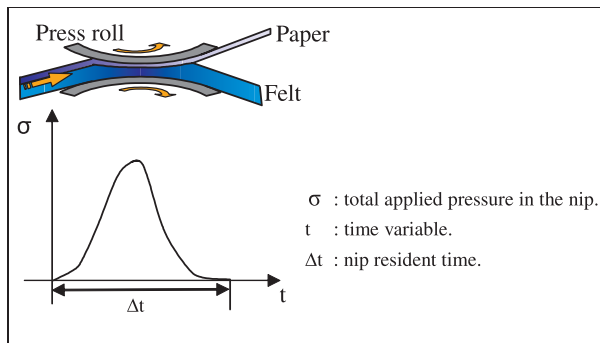


Figure 1 Schematic view of a press nip in paper process.

the press nips, both paper and felt are compressed between two rolls (Figure 1). The deformation leads to a dramatic increase in hydraulic pressure. As this hydraulic pressure gradient exists in the press nip, a water flow occurs.

With the improvements of the felt making process, using new raw materials such as synthetic fibers, and new felt design (double and triple base weave), it is necessary to characterise the new products. Therefore, the flow resistance measurement will help to give a better understanding not only of the physical mechanisms in the press nip but also of felt design.

Considering classical pressing conditions, especially temperature and pressure, the water may be considered as an incompressible Newtonian fluid. Hence, at the microscopic level (the fiber scale), the liquid flow may be described by the Navier-Stokes equation. The time dependency of equations vanishes, as the speed variations of the paper machine production are negligible (steady-state condition). On the other hand, the viscous forces are classically considered to be much larger than the inertial forces [1]. Thus, the momentum equation corresponding to the steady-state Stokes equation (equation (1)) may be written as follows:

$$-\mathbf{grad}(P) + \mu \Delta \mathbf{v} = \mathbf{0} \quad (1)$$

where P is the pressure, \mathbf{v} the velocity vector, μ the kinematics viscosity.

At the macroscopic level, the relationship between the velocity and the pressure P , is considered to follow Darcy's law (equation (2)).

$$\langle \mathbf{v} \rangle = -\frac{1}{\mu} \mathbf{K} \langle \mathbf{grad}(P) \rangle \quad (2)$$

where $\langle X \rangle = \frac{1}{|\Omega_k|} \int_{\Omega_k} X d\Omega$, in which Ω_k is the considered volume for the mean calculation.

In order to optimise a press section, models taking into account the considered technology may be used [2–5]. The results of these models will be in good agreement with reality only if the physical properties of the different components of the press section are known quantitatively (e.g. roll resilience, felt resilience, felt permeability). Keeping in mind these main aims, this paper deals with the permeability measurement of strained press felt.

This paper is divided into four parts. The first is focused on the experimental device used for the permeability measurements. The second deals with the description of the experimental protocol. Results and discussion are exposed in the third part. In the last part, a conclusion will end this paper.

Description of the Experimental Device

In the literature [4, 6–8], when studying the flow through a press nip, the flow in the thickness direction is considered as the most important for the process efficiency. Nevertheless, in order for the pressing operation to be accurately modeled, the flow in the press section has to be considered in three spatial directions. During this process, the felt is strained by the compression. Furthermore, the felt is tightened in order to drive the non-motorised rolls. Therefore it is important to determine the flow resistance for different levels of felt strain.

The transverse flow cell is briefly described in the next subpart. The second subpart focuses on the device that allows characterisation of the in-plane permeability tensor of press felt. Water has been used in our experiments in order to avoid any problem due to fluid compressibility, as may be the case with gas.

The Transverse Flow Cell

Classically, in such an experimental device, the flow is imposed orthogonal to the felt plane. The pressure drop created by the felt is related to the seepage velocity of the fluid. The device we used in previous work (Figure 2) is presented in detail in reference [9]. No sealing of the cell is realised in order for this equipment to measure permeability of felt installed on machines. A guard ring is used to measure the flow not affected by the leakage. Therefore, such an apparatus allows flow resistance measurement of felt that is at the same time compressed and tightened.

The In-Plane Flow Cell

The flow resistance of non-woven textile is studied in various domains such as medicine or geomechanics. Different

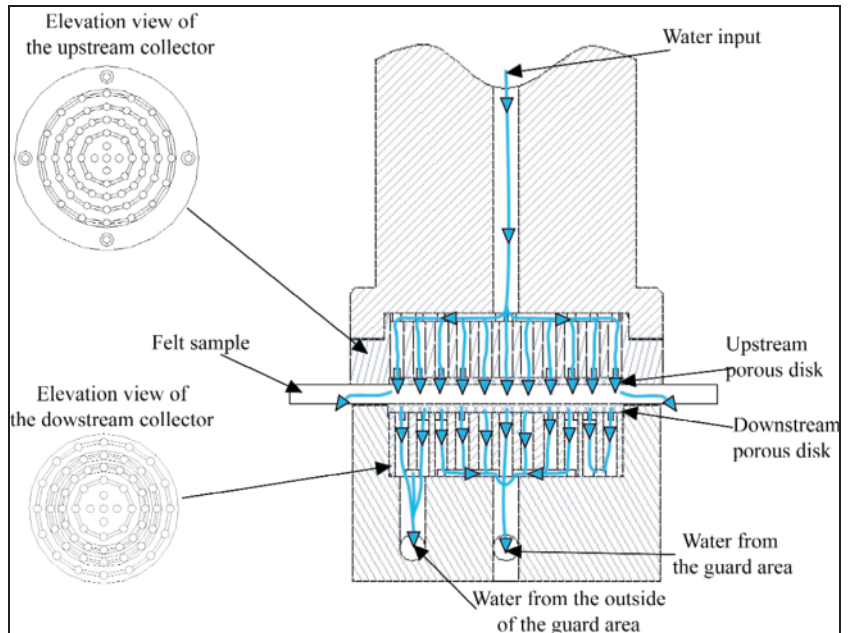


Figure 2 Schematic view of the experimental cell used to measure the transverse permeability.

experimental techniques have been used. They may be classified with respect to the used fluid (liquid or gas) and the flow direction (radial flow or unidirectional flow, see Figure 3). For example, in the resin moulding process, a woven or non-woven textile is placed inside a mould. In this industrial field of resin moulding, numerous undertakings have been conducted to study the permeability anisotropy of fiber beds. These works deal with both radial flow and unidirectional flow techniques. In the first method, the fluid is injected in the center of the sample. The progression front is correlated to the pressure injection. This method leads to direct evaluation of the flow resistance tensor. In the second method, the fluid is canalised and flows in only one direction. Therefore, the flow permeability is measured in this direction only. Several studies, such as Lekakou et al.'s work [10], compare flow resistance measurements using both techniques considering glass fiber beds with porosities (equation (3)) larger than 0.4. With the unidirectional method the measurements are one order of magnitude higher than with the radial method. The fluid front progression inside the porous media is found to be well described by Darcy's law. However the permeability depends on the flow rate. Hence the proposed model is nonlinear. According to the author, the nonlinear phenomenon is created by the fibrous bed strain.

$$\varepsilon = \frac{V_v}{V_t}; \quad \varepsilon = 1 - \frac{W}{\rho_f \cdot e} \quad (3)$$

where ε , V_v , V_t , ρ_f and e represent respectively the porosity, the void volume, the total volume of material, the fiber density and the thickness.

Parnas [11, 12] finds similar results using both techniques. The porosity of the tested non-woven media ranges from 0.8 to 0.45. The corresponding permeability measurements gap between 100 and 1 μm^2 . However, it has to be underlined that the main directions of the permeability tensor of the tested textile are not the same as the main directions of the structure. Gebart [13] comes to the same conclusion. Notwithstanding, he shows that the radial flow technique may be erroneously influenced by the deformation of the apparatus. Then, Lundström [14] shows that as the porosity of tested fibrous media ranges from 0.7 to 0.5, the permeability decreases from 150 to 17 μm^2 . Moreover, as the radial flow technique is based on the observation of the fluid front, only transparent media may be used for the apparatus design. This is a major limiting factor for the choice of the raw material (generally made of Plexiglas). Nevertheless, original methods based on the radial flow technique exist using either optic fibers [15] or thermocouples [16]. With such methods, there is no need for any visualisation of the flow. Hence, the frame of the apparatuses may be made of stiffer raw materials.

Existing devices that measure the in-plane flow resistance of papermaking press felt are based on unidirectional flow. Generally, felt flow resistance is measured in one direction corresponding to the paper machine direction and sometimes in the cross machine direction. Macklem carried out first studies on press-felt permeability [17]. Porosity of wool-made felt under compression ranges from 0.7 to 0.3 and the corresponding in-plane permeability ranged from 67.4 to 0.1 μm^2 . Kershaw [18] conducted a similar work on felt with mixed synthetic wool fibers. Porosity of such felt under compression ranges from 0.8 to 0.6 and the corre-

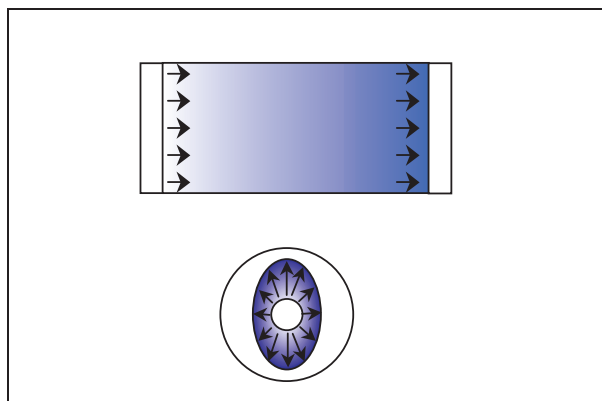


Figure 3 Illustration of devices using in-plane unidirectional (top) and radial (bottom) flow.

sponding in-plane permeability ranges from 100 to 50 μm^2 . Ballard [19] and later Chevallier [20] completed this work, taking into account the tension influence and studied felts made only of synthetic raw materials. Porosity ranged from 0.6 to 0.3 and permeability from 100 to 1 μm^2 . Finally, Lundström et al. [21] and later Thibault [9] measured felt flow resistance of modern felts.

In the preceding paragraph, the unidirectional and radial techniques were shown to be equivalent. However, the experimental conditions associated with the radial tech-

nique have to be carefully controlled especially the deformation of the structure of the apparatus. Regarding the stress level during pressing, the unidirectional flow method is more adapted to the context of this study. In order to avoid adventitious strain of the felt, the cell is not sealed. The flow in the felt plane is imposed using three parallel slits. The hydraulic pressure in the external slits is higher than in the central one. Thus, the designed cell imposes a flow through the felt plane from the external slits to the central one (Figure 4). These slits may be orientated in any direction of the plane.

A guard area is used to take into account only the flow that is not influenced by the boundary conditions. Indeed, the water flow inside this area is used to perform flow resistance measurements. The flow inside the cell was previously simulated using Matlab[®] to check the efficiency of the chosen design. Darcy's equation and mass conservation were used in order to evaluate the pressure gradient. The chosen geometry was a horizontal cross section of the cell. This numerical investigation showed that the flow inside a central part of the cell was not influenced by the outside boundary conditions (Figure 5). Furthermore, assuming that the in-plane flow resistance was lower or equal to the transversal one, the in-plane flow stream was 20 times longer than the transversal one. Preliminary work was carried out on transverse flow resistance, which validated this assumption [22].

The flow resistance measurement device is 240 mm high \times 205 mm long \times 166 mm large. It is made of stainless steel. The total cell diameter is 120 mm large. The

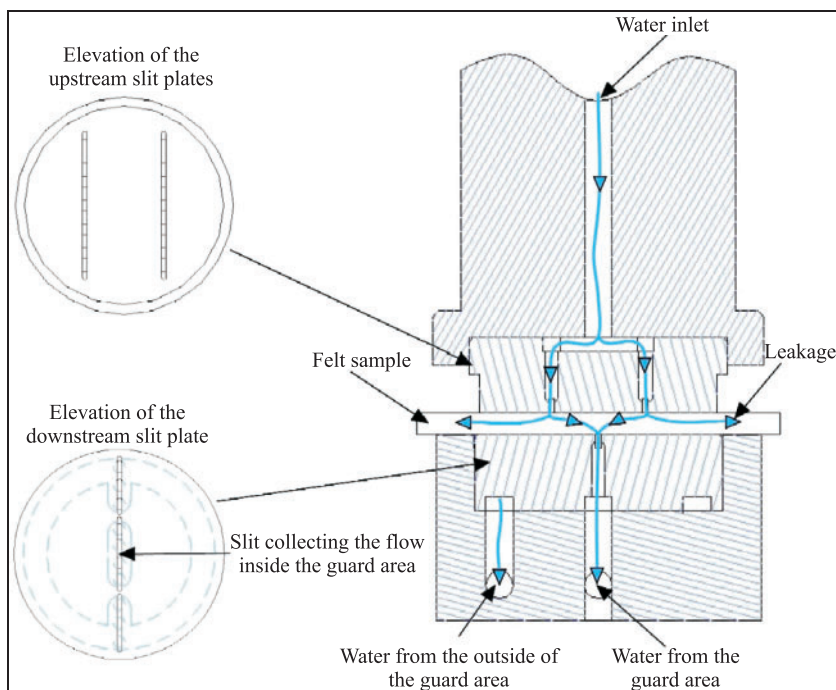


Figure 4 Flow in the apparatus cell. The view of this section is perpendicular to the slits.

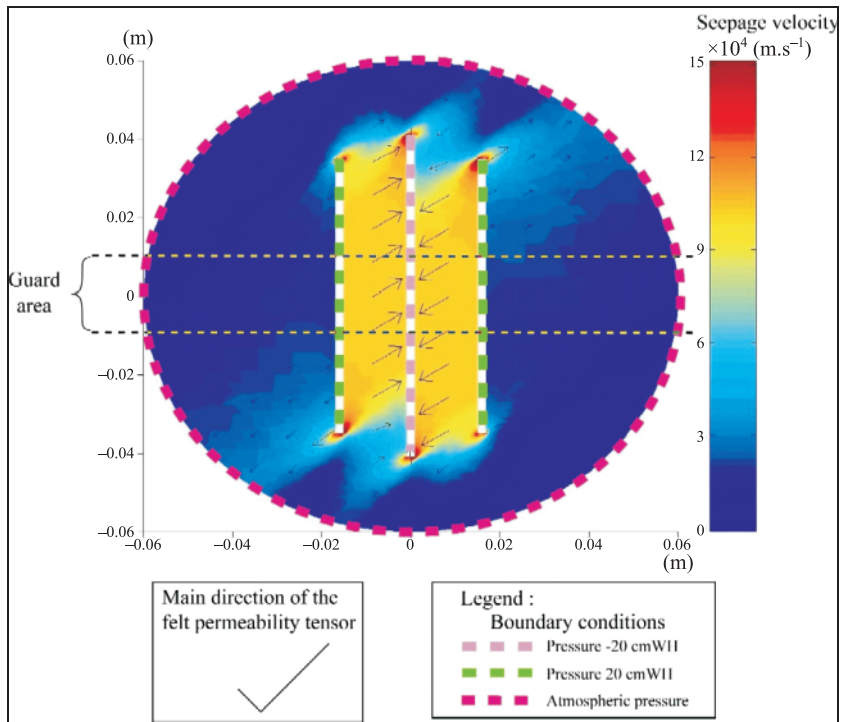


Figure 5 Pressure field inside the in-plane permeability cell (simulated with Matlab®) for an applied pressure of 20 cm water.

whole device is compressed using a pneumatic jack. The force applied on the device may reach 60 kN, which corresponds to a mechanical stress on the felt of 6 MPa. A frame is used to tighten the felt up to a tension of 1200 daN.m⁻¹. This frame is placed in the felt plane. Typically on a paper machine, the compressive stress on the felt may reach 6 to 10 MPa and felt tension about 700 daN.m⁻¹.

Three tanks, one upstream and two downstream, are used to impose a constant pressure gradient inside the felt (Figure 6). The maximum height between upstream and downstream vases is 2 m. This corresponds to a maximum pressure loss of 20 kPa. The vase heights are measured with a vertical scale; the accuracy is 1 mm. Hence, the

measurement error on the pressure loss is 20 Pa. Higher pressure drop [400 kPa] may be reached using a water network. The position of the upper part of the compressing device is measured with a LVDT displacement captor. This allows the evaluation of the felt thickness with an accuracy of 20 μm for a thickness of 2 mm.

To test the efficiency of the guard area, two preliminary experiments were performed. The first was conducted under standard conditions, i.e. allowing lateral leakage (water flow that goes outside the cell without pouring the downstream tanks) and introducing a felt. The second was carried out on the same felt without any leakage. The results are presented in Figure 7. The both resulting curves

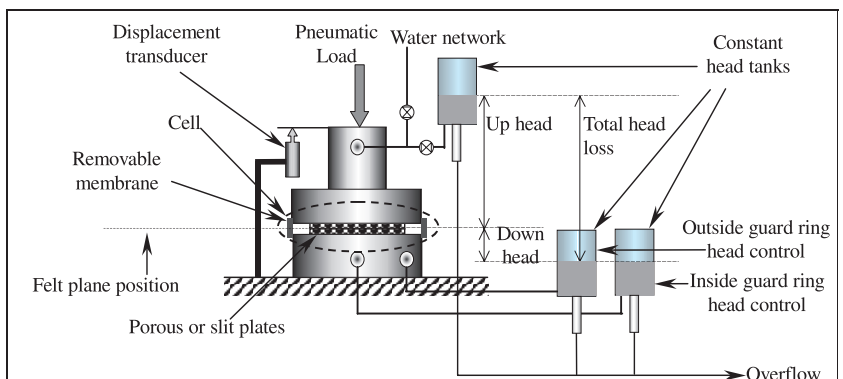


Figure 6 Schematic diagram of the permeameter equipment.

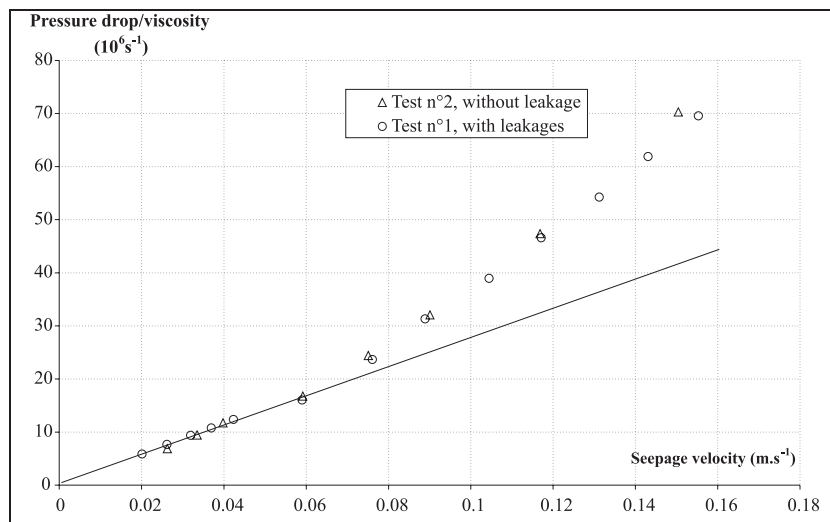


Figure 7 Comparison of the ratio of the head loss of the device with a sample to the water viscosity versus the seepage velocity.

are very close this leads to the conclusion that the guard area is efficient.

These results also justify the use of Darcy's law due to the linearity of the relationship between the ratio pressure drop – viscosity and the seepage velocity inside the guard area when the pressure drop is smaller than 20 kPa.

Experimental Procedures

In order to evaluate the appearance of nonlinearities due to, for example, the presence of bubbles in the liquid, the “water network” was used. The water is stocked in a tank 24 hours before its use in the experiment, in order for dissolved air in the liquid to reach a steady concentration. Hence, no air bubbles are expected to appear and consequently the flow is monophasic. Furthermore, 24 hours before the experiments, the felt sample is saturated with water. For each felt, no swelling effect has been noticed. In this article, results related to transverse and in-plane permeability measurements are presented.

The relationship between the pressure drop and the flow rate of the apparatus without any felt sample is initially studied. In the case of the in-plane permeability cell, this pressure drop is found to be negligible compared to the one due to the felt. This is not the case for transverse permeability. Hence the relationship between the pressure drop and the flow rate of the apparatus without any felt is taken into account when evaluating the transverse permeability.

Before any measurements, the cell is compressed without any sample in order to determine the deformation of the experimental apparatus under stress. Afterwards, a felt sample is introduced into the cell, which is tightened to a

chosen stress level. Next, the felt is compressed to a chosen stress level. After the felt creep (15 to 20 minutes), the relationship between the pressure drop and the flow rate is evaluated and the temperature is measured. Indeed, temperature variations are taken into account in the evaluation of the water viscosity. Each measurement is made under steady-state conditions regarding the saturated felt compression and the water flow conditions. The linearity, and thus the validity of Darcy's law, is verified for all measurements. The pressure drop (ΔP) versus the flow rate relationship is obtained using the least square regression method involving at least four experimental points for any strain level. The uncertainty range is computed for each permeability evaluation. When measuring the in-plane permeability, the direction of the flow is evaluated using the slit marks on the felt batt obtained just after the compression.

Results and Discussion

Felt Sample Features

The flow resistance investigation of four different felts is presented in this paper. Some characteristics of these samples are presented to demonstrate the efficiency of the equipment for different felt structures (Table 1). The differences between felts C-1 to C-4 are mainly in the orientation of their batt fibers. The batt fibers of C-1 are oriented in the cross machine direction. C-2 ones are isotropic oriented. C-3 ones are oriented in the machine direction. Finally, C-4 batt is constituted by a successive matt of fibers oriented $\pm 45^\circ$ relatively to the machine direction.

The classical Kozeny-Carman's relationship (equation (4)) and an exponential law (equation (5)) were used to

Table 1 Description of the tested felt structures illustrated with a tomographic reconstruction of a single base weave felt (C-4).

Sample	Basis weight	Base	Batt	Base yarns diameter	Batt fibers average diameter
	kg/m ²			mm	μm
C-1	1100	380	720	Single base	31
C-2				weave	
C-3				MD ⁽¹⁾ 6 × 0.20	
C-4				CMD ⁽²⁾ 0.40	

(1) MD: paper Machine Direction
 (2) CMD: Cross Machine Direction

analyze the experimental results concerning the transverse permeability of felt in previous work [9]. In this work, the exponential law was also found to fit better the experimental results than Kozeny-Carman’s law. However the main drawback of such a law is that as the porosity tends to zero, the permeability tends to a non-zero value. A power law (equation (6)) is also used here to fit the experimental results.

$$K = \frac{\varepsilon^3}{k_o \tau^2 S_v^2} \tag{4}$$

$$K = \Lambda \cdot 10^{\Psi \varepsilon} \tag{5}$$

$$K = \alpha \cdot \varepsilon^\beta \tag{6}$$

where ε , K , τ and S_v represent the porosity, the permeability, the tortuosity and the specific volume surface, respectively. k_o , α , β , Λ and Ψ are parameters.

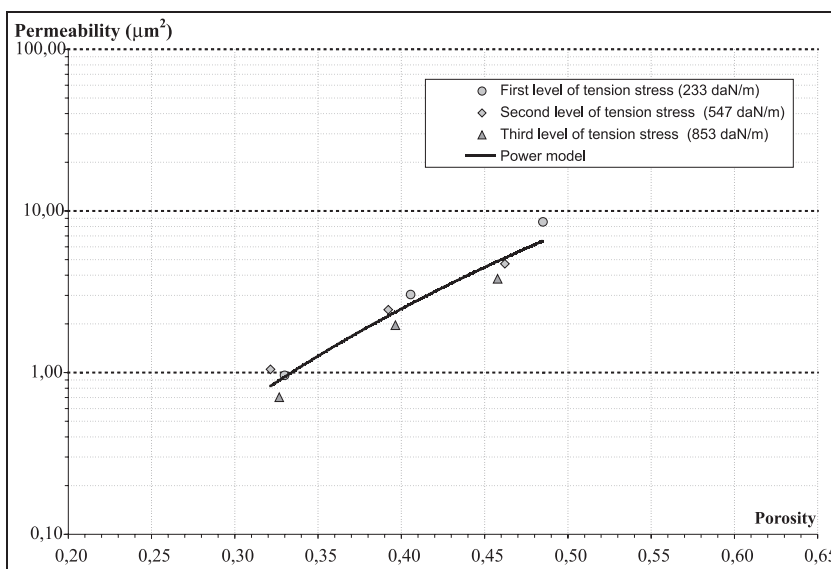
First, results on transverse permeability are presented. Secondly, those concerning in-plane permeability are exposed.

Transverse Permeability

Before the compression step, the felt sample is tightened in the paper machine direction to one of the three tension levels: 2,33 kN.m⁻¹, 5,47 kN.m⁻¹ or 8,53 kN.m⁻¹. After each step of tightening, the relationship between felt compression and its permeability is studied. The compression stresses are identical for all performed experiments. The successive levels of compression are 0.4 MPa, 1.6 MPa and 4.7 MPa.

When the compression increases, the transverse permeability decreases monotonously (Figures 8 to 11). A power

Figure 8 Felt C-1 transverse permeability versus porosity.



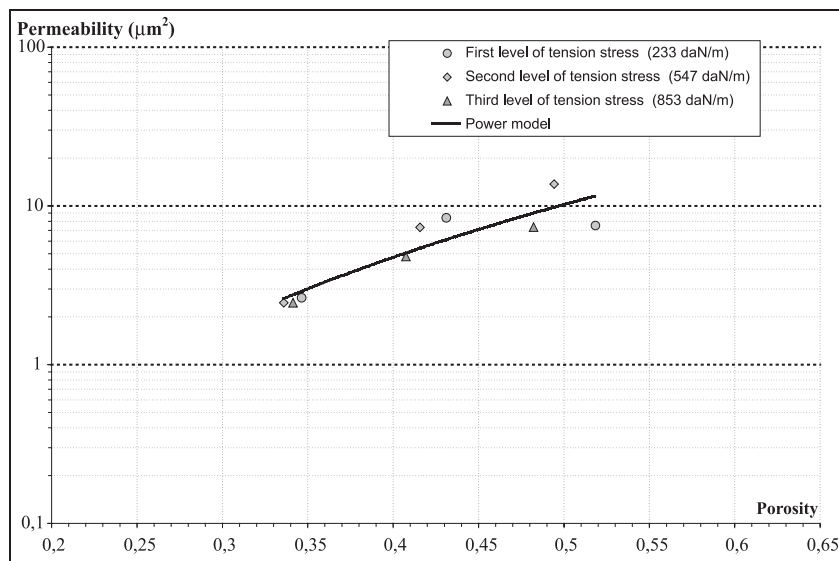


Figure 9 Felt C-2 transverse permeability versus porosity.

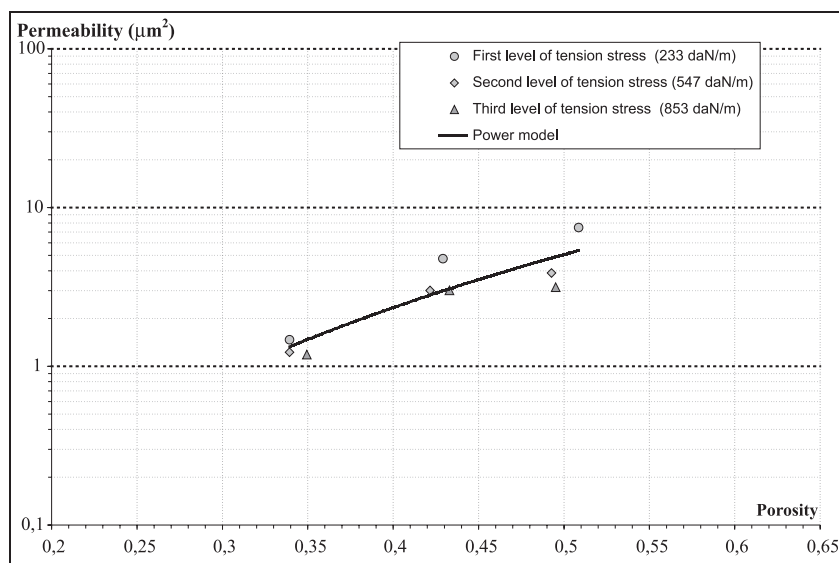


Figure 10 Felt C-3 transverse permeability versus porosity.

relationship correctly fits all the experimental results (equation (6)). Fitting results are presented in Table 2. In order to compare felt permeability behavior, the permeability is related to porosity.

The felt tension has no significant influence either on its compressibility or on permeability. Only the compression strain modifies the permeability. The woven base of the felt increases dramatically the rigidity in the machine direction. Hence, minor structural strains are allowed when the felt is tensioned. Therefore, the permeability remains almost constant. On the contrary, in the thickness direction batts are compressible compared to the base. When compressed, the

felt porosity decrease is mainly due to the batt fibers. This aspect was pointed out in [23].

The influence of the fiber orientation on the permeability reveals that the isotropic batts (C-2 felt) present the smallest flow resistance (Figure 9), whereas the stratified structure (C-4) presents the largest flow resistance (Figure 11). This is interesting as the C-4 felt has a higher porosity than the C-2 felt. Orientated batt fibers either in MD (C-3, Figure 10) or CMD (C-1, Figure 8) have no significant influence on the transverse permeability. Nevertheless, porosity is slightly higher for the felt C-3.

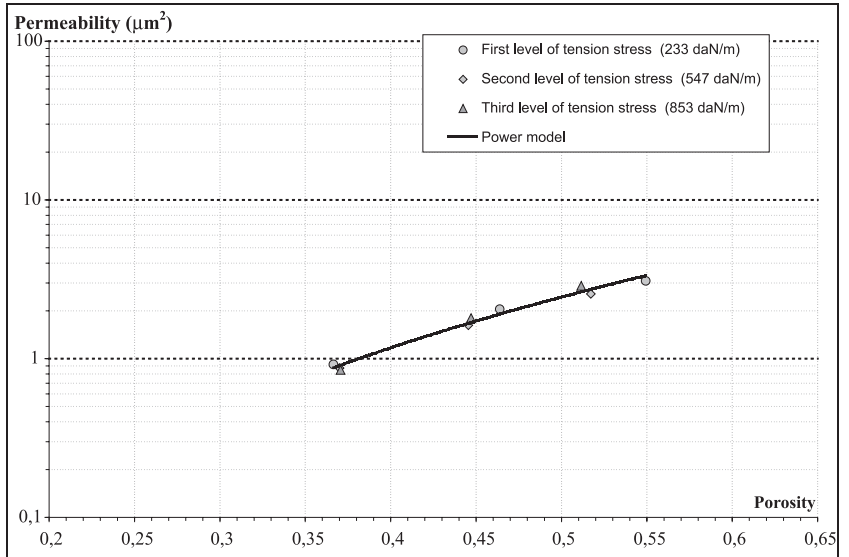


Figure 11 Felt C-4 transverse permeability versus porosity.

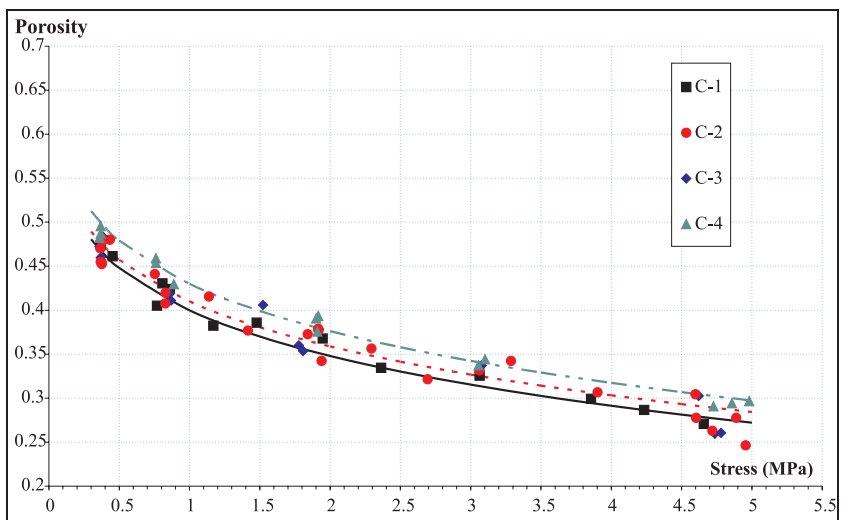


Figure 12 Porosity versus applied stress. Each trend line is the result of fitting with the two parameters (A and B) law: $\varepsilon = 1 - A\sigma^B$.

In-plane permeability

All felts were compressed to stresses ranging from 0.5 to 6 MPa. The corresponding porosity evaluated from the thickness measurements ranged from 0.65 to 0.25. The felt rheology (that is to say, the relationship between porosity and applied stress) is shown in Figure 12. This result confirms that the felt C-4 has a higher porosity than other felts no matter what the compression level is.

For each type of felt, the in-plane permeability is measured in three different directions: machine direction (MD), cross direction (perpendicular to MD) and 45° relatively to the MD. After measuring permeability in one direction the felt sample is removed and is replaced by a new one. Experimental results show that the in-plane per-

meability tensor is isotropic for all tested felt (Figures 13 to 16). C-type felts present similar permeability behavior in respect to porosity. Fiber orientation does not seem to affect the in-plane permeability tensor component either in anisotropy or in the evolution in respect to compression. The power relationship between the porosity and the permeability fits the experimental results either in the transverse direction or in any in-plane directions.

The tension dependence of the in-plane permeability is only presented for the C-1 sample in the machine direction because all in-plane permeability measurements of felt were found to be similar. The measurements show identical results as in the previous permeability study (Figures 13 to 16). Contrary to the idea proposed in literature [20], the tension stress has no significant influence on the permeability tensor.

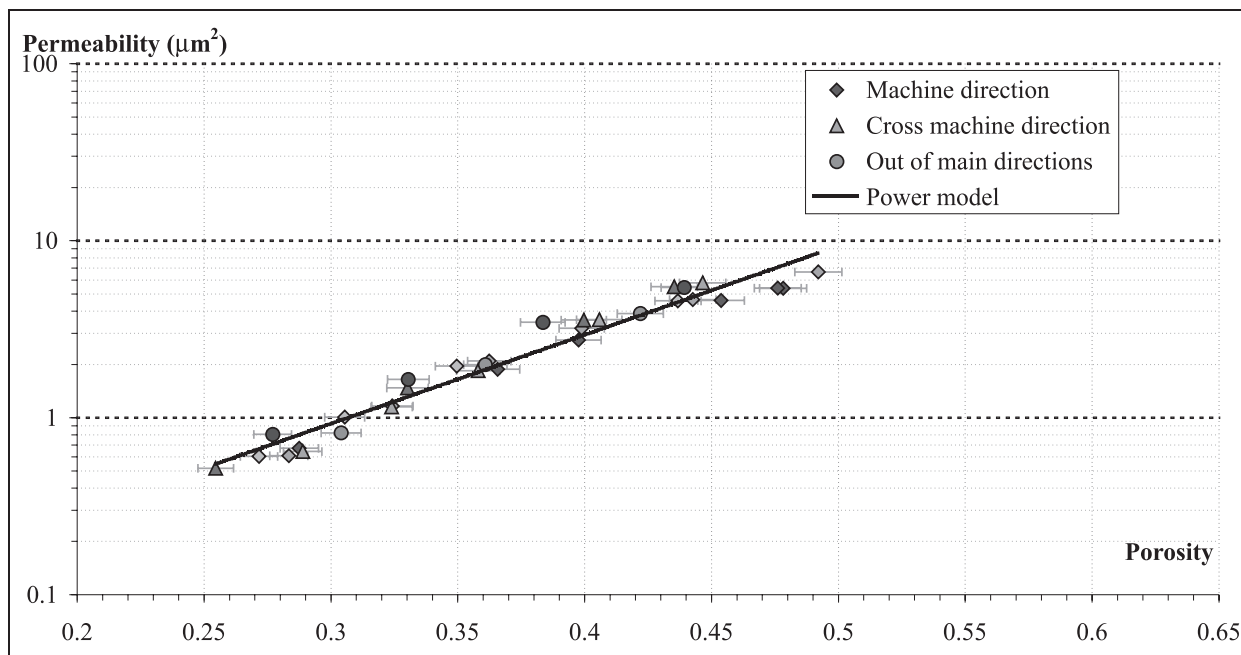


Figure 13 C-1 in-plane permeability evolution with the felt compression.

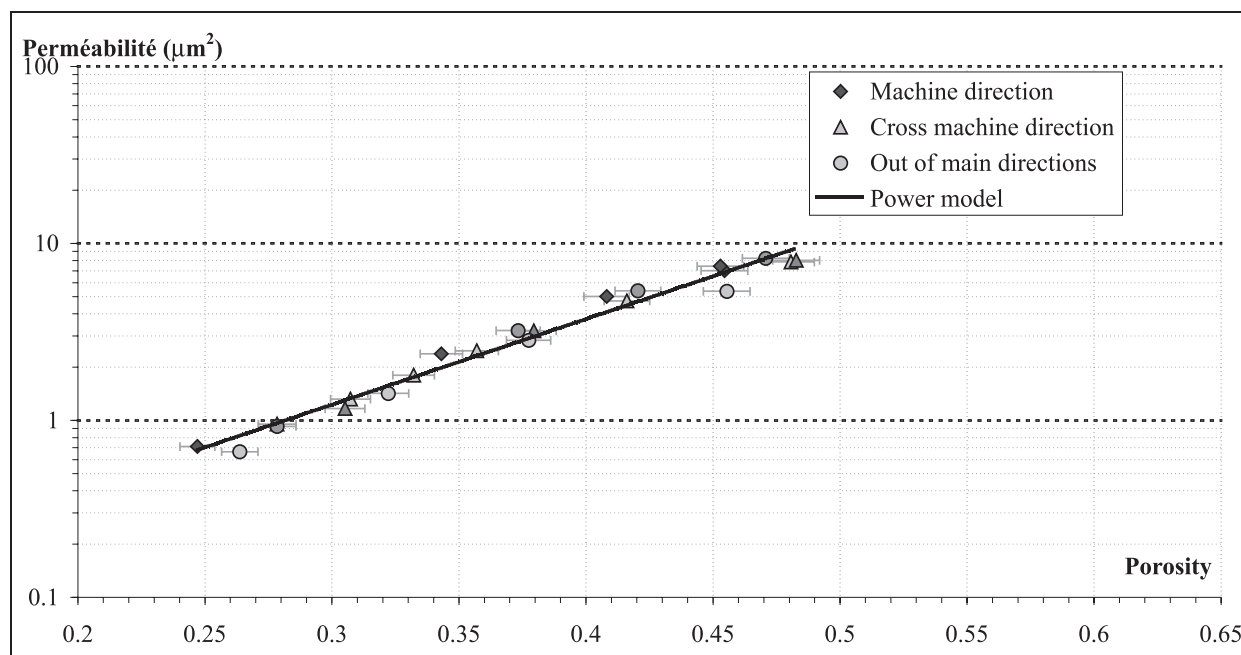


Figure 14 C-2 in-plane permeability evolution with the felt compression.

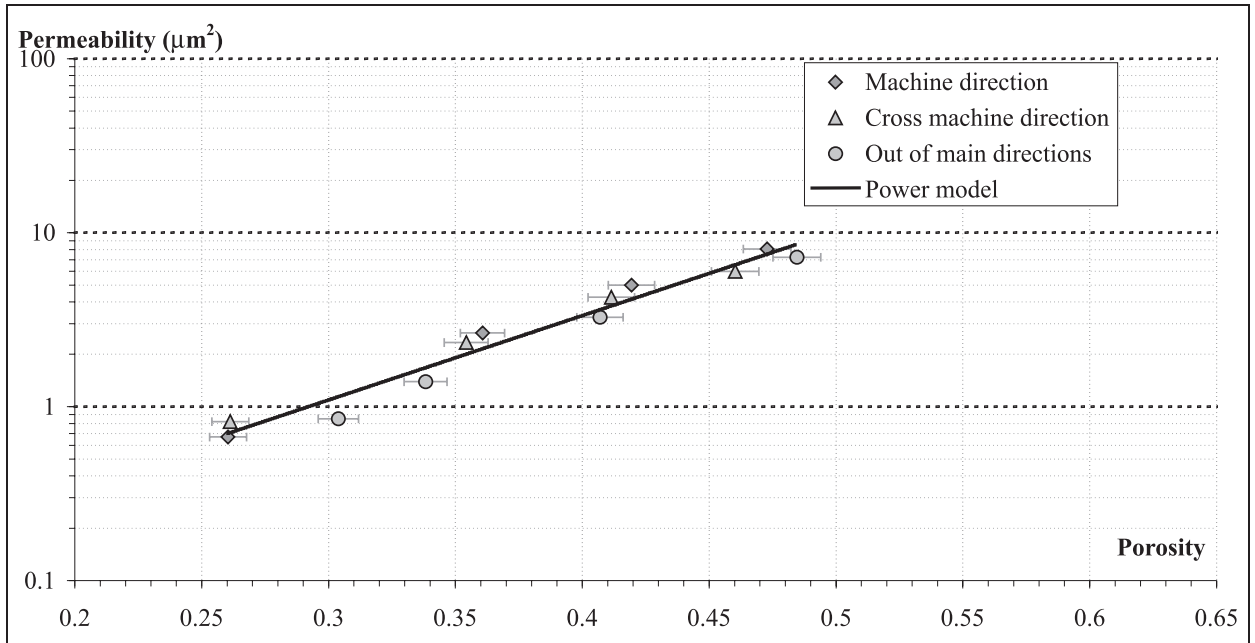


Figure 15 C-3 in-plane permeability evolution with the felt compression.

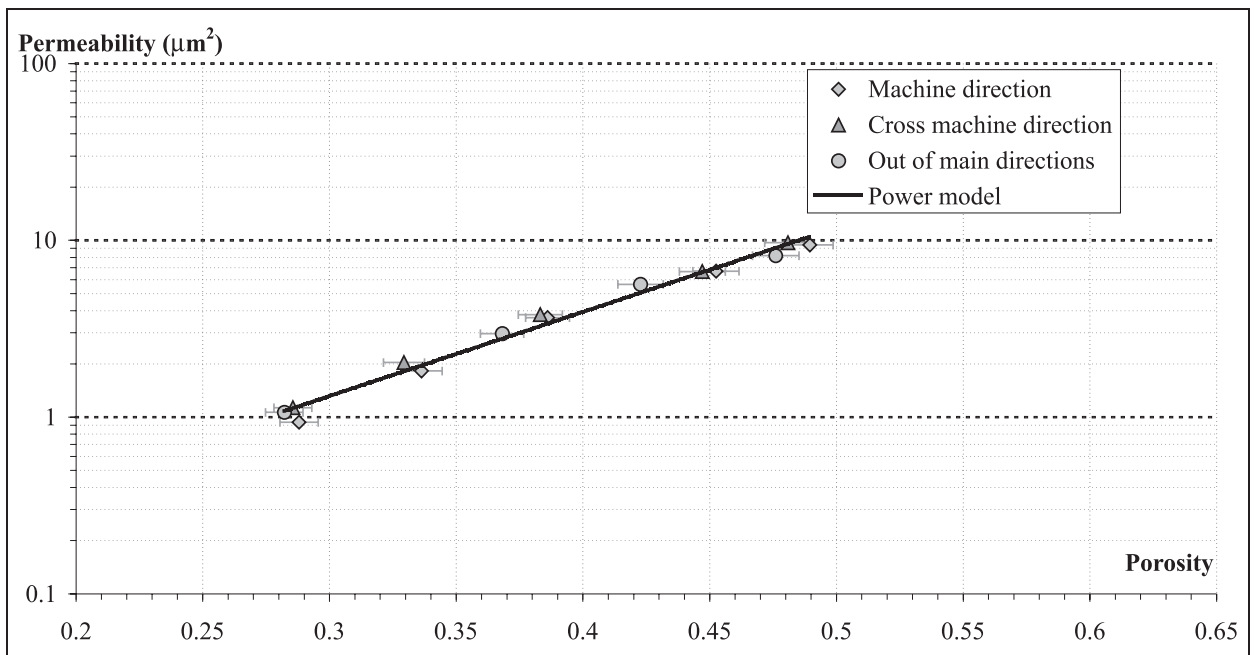


Figure 16 C-4 in-plane permeability evolution with the felt compression.

Table 2 Identification of the power laws (equation (6)) for the different felts.

Felt	Permeability	Model (μm^2)	R ²	Validity domain
C1	Transverse	$247.82 \cdot \epsilon^{5.027}$	0.941	0.32–0.49
	In-plane	$150.25 \cdot \epsilon^{4.230}$	0.971	0.25–0.49
C2	Transverse	$109.72 \cdot \epsilon^{3.427}$	0.822	0.34–0.51
	In-plane	$159.03 \cdot \epsilon^{4.026}$	0.984	0.25–0.48
C3	Transverse	$55.33 \cdot \epsilon^{3.451}$	0.801	0.34–0.50
	In-plane	$140.91 \cdot \epsilon^{4.016}$	0.961	0.26–0.48
C4	Transverse	$24.02 \cdot \epsilon^{3.297}$	0.983	0.37–0.55
	In-plane	$186.01 \cdot \epsilon^{4.131}$	0.992	0.28–0.49

Table 3 Permeability evaluation at a given porosity ($\epsilon = 0.4$) for the different felts.

Felt	Permeability	Model (μm^2)
C1	Transverse	0.990
	In-plane	3.115
C2	Transverse	4.748
	In-plane	3.975
C3	Transverse	2.342
	In-plane	3.555
C4	Transverse	1.171
	In-plane	4.223

Table 3 illustrates the differences between the felt permeabilities. The respective permeabilities were calculated for a given porosity ($\epsilon = 0.4$) from the expression presented in Table 2.

Conclusion

In order to optimise a paper press section a felt has to be chosen. Classically this choice is made in respect to the unstrained felt transverse permeability. On the other hand, numerical models of the paper pressing process need data to take into account the felt permeabilities evolution during the pressing operation. The experimental device described in this paper allows the investigation of the permeability tensor of strained fibrous media.

First, the measured permeability values agree with the values classically found in the literature. The presented results show that structure orientation does not signifi-

cantly influence in-plane flow resistance. Nevertheless, the permeability is higher in the thickness direction when batt fibers are not oriented. To establish a numerical model, the power model fits correctly to the behavior of permeability in respect to the porosity.

The presented equipment is also useful for other kinds of materials involved in different industrial sectors in which the evaluation of the permeability tensor for various strained states has to be known to improve the knowledge and therefore the efficiency of the considered industrial operation.

Acknowledgment

This work was carried out in the context of the European project JOULE III (JOECT92). Albany Nordiskafilt is especially thanked for providing the presented felt samples. The authors would like to thank Y. Chave, J.-M. Serra-Tosio, and all the people who helped in the writing of this paper. In particular, we are very grateful to R. Sen for his help concerning the English language.

Literature Cited

- Roux, J. C., Modélisation et optimisation du fonctionnement des presses de machines à papier. *Récent Progrès en Génie des Procédés*, **1**, 223–228 (1987).
- Skelton, J. and Toney, M. M., A Computer Model of a Roll Press Nip, *TAPPI J.*, **84**, 1–14 (2001).
- Jewett, B. K., “The Application of a Model for Two Phase Flow Through a Compressible Porous Media to the Wet Pressing of Paper,” PhD, University of Maine, Orono, 1984.
- MacDonald, J. and Kerekes, R. J., A Decreasing Permeability Model of Wet Pressing with Rewetting, *TAPPI J.*, **78**, 107–111 (1995).
- Gustafsson, J.-E. and Kaul, V., A General Model of Deformation and Flow in Wet Webs under Compression. *Nordic Pulp and Paper Res. J.*, **16**, 149–154, (2001).
- Wahlström, B. J., Our Present Understanding of the Fundamentals of Pressing. *Pulp and Paper Magazine of Canada* **70**, 76–96 (1969).
- MacDonald, J. D., Hamel, J., Kerekes, R. J., Design Equation for Paper Machine Press Sections, *J. Pulp and Paper Sci.*, **26**(11), 401–406 (2000).
- Asklöf, C., Larsson, K., Linderöth, J., and Wahlström, P., Flow Conditions in a Felt in a Plain Press Nip, *Pulp and Paper Magazine of Canada*, T246–T250 (1964).
- Thibault, X., Bloch, J.-F., Chave, Y., Serra-Tosio, J. M., Measurements of the Permeability of Press Felts, *Paperi ja puu*, **86**(2), 95–101 (2004).
- Lekakou, C., Johari, M. A., Norman, D., and Bader, M., Measurement Techniques and Effects on In-Plane Permeability of Woven Cloths in Resin Transfer Moulding, *Comp. Part A*, 401–408 (1996).
- Parnas, R. S., Howard, G. J., Luce, T. L. and Advani, S. G. Permeability Characterisation. Part I: A Proposed Standard

- Reference Fabric for Permeability, *Polym. Comp.*, **16**, 429–445 (1995).
12. Parnas, R. S. and Salem, A. J., A Comparison of the Unidirectional and Radial In-Plane Flow Through Woven Composite Reinforcement, *Polym. Comp.*, **14**, 383–394 (1993).
 13. Gebart, R. B. and Lidström, P., Measurement of In-Plane Permeability of Anisotropic Fiber Reinforcements, *Polym. Comp.*, **16**, 429–445 (1996).
 14. Lundström, T., Stenberg, R., Bergström, R., Partanen, H., and Birkeland, P., In Plane Permeability Measurements: A Nordic Round Robin Study, *Composites Part A*, 29–43 (2000).
 15. Ahn, S. H., Lee, W. I., and Springer, G. S., Measurement of the Three-Dimensional Permeability of Fiber Preforms using Embedded Fiber Optic Sensors, *J. Comp. Mat.*, **29**, 714–733 (1995).
 16. Weitzenböck, J., Sheno, R., and Wilson, P., Measurement of the Three-Dimensional Permeability, *Comp. Part A*, 159–169 (1998).
 17. Macklem, J. E. A Study of the Resistance of Woven Wool Felts to Liquid Flow, *TAPPI J.*, **44**, 535–544 (1961).
 18. Kershaw, T. N., The Three Dimensions of Water Flow in Press Felts, *TAPPI J.*, **55** 880 – 887 (1972).
 19. Ballard, J., Press Felt Characterization, in *TAPPI Engineering Conference*, Atlanta, pp. 117–122, 1986.
 20. Chevallier, P., Felt Design Factor: A Tool for Optimizing Sheet Dryness, in *TAPPI Engineering Conference*, Boston, 1992.
 21. Lundström, S. T., Gebart, R. B., and Sandlund, E., In-Plane Permeability Measurements on Fiber Reinforcements by Multi-Cavity Parallel Flow Technique, *Polym. Comp.*, **20**, 146–154 (1999).
 22. Thibault, X. and Bloch, J.-F., Permeability Measurement of Strained Felt: Application to Paper Making Process, in *8th World Filtration Congress*, Brighton, 1011–1014, 2000.
 23. Thibault, X. and Bloch, J.-F., Structure Analysis by X-ray Microtomography of a Strained Non-woven Papermaker Felt, *Text. Res. J.*, **72**, 480–485 (2002).